

# Characterization of cellulose crystallinity after enzymatic treatment using Fourier transform infrared spectroscopy (FTIR)

Nathan Kruer-Zerhusen · Borja Cantero-Tubilla · David B. Wilson

Received: 13 April 2017 / Accepted: 28 October 2017  
© Springer Science+Business Media B.V., part of Springer Nature 2017

**Abstract** Cellulase activity on insoluble cellulose substrates declines as the substrate is modified. The role of structural changes that result in substrate recalcitrance, such as changes to cellulose crystallinity, requires further investigation. Crystallinity of cellulose samples with varying extents of digestion can only be compared meaningfully using a high throughput - Fourier transform infrared spectroscopy (HTS-FTIR) technique when the many variables involved are carefully controlled. Hence, changes to the HTS-FTIR sample preparation methods previously described in literature were necessary in order to obtain clean raw spectra and reliable measures of cellulose crystallinity. The sample preparation methods of residual cellulose after digestion by individual

cellulases and a complex cellulase mixture from *T. fusca* were improved to remove extraneous overlapping signals, provide accurate extent of digestion, and correct errors caused by varying concentrations. These improved preparation methods enabled measurement of crystallinity index values of residual cellulose which did not show a correlation between cellulose crystallinity and the decline in cellulase activity.

**Keywords** Cellulose Crystallinity · Recalcitrance · Cellulase · *Thermobifida fusca* · Fourier Transform Infrared (FTIR) spectroscopy · Crystallinity indexes

---

First and second author contributed equally to this work. This work is dedicated to the memory of Prof. David Wilson.

---

**Electronic supplementary material** The online version of this article (<https://doi.org/10.1007/s10570-017-1542-0>) contains supplementary material, which is available to authorized users.

---

N. Kruer-Zerhusen · D. B. Wilson  
Department of Molecular Biology and Genetics, Cornell University, Ithaca, NY 14853, USA

B. Cantero-Tubilla (✉)  
Robert Frederick Smith School of Chemical and Biomolecular Engineering, Cornell University, Ithaca, NY 14853, USA  
e-mail: bc497@cornell.edu

## Introduction

Cellulosic biomass is an abundant and sustainable resource that has the potential to be a significant component of a carbon-neutral energy system. Carbohydrates obtained from the breakdown of biomass can be utilized by various microorganisms to produce alcohols or combustible hydrocarbons for use as transportation fuels. The bottle-neck in the development of an efficient and economically feasible system to produce biomass fuels is the limited yield of enzymatic hydrolysis of cellulose by cellulases (Kostylev and Wilson 2011). The digestion of insoluble cellulose is a complex process because of the multiple enzymatic steps required for cleavage, and the heterogeneity of the substrate, which changes

during the reaction. A constant rate of hydrolysis is never achieved during cellulose digestion, and the rate begins to drop off rapidly after the initial digestion. A decrease in substrate reactivity with the extent of substrate digestion has been demonstrated, although the exact reasons for this behavior are not easily determined (Kostylev and Wilson 2013).

Cellulose is a recalcitrant crystalline lattice of closely packed polysaccharide chains, linked by an extensive hydrogen bonding network. Substrate recalcitrance is the combination of physical and chemical factors that contribute to reduced cellulase activity. Cellulases modify the cellulose substrate during digestion, and the impact of these structural changes on kinetics is not well understood (Kostylev and Wilson 2013; Våljamäe et al. 2003; Xu and Ding 2007). Cellulose crystallinity, the degree of organization of the cellulose lattice, is believed to play a major role in the activity of most cellulases. It is correlated with more stable cellulose (Lionetto et al. 2012). Although it is a commonly held hypothesis, the link between changes in cellulose crystallinity and extent of digestion has not been conclusively established by existing work. Two hypotheses of the role of crystallinity in substrate recalcitrance have been investigated. Increasing cellulose crystallinity over the course of digestion is an intuitive hypothesis; crystalline regions are more difficult to degrade, so as cellulases preferentially target the less ordered chains the crystalline regions become more abundant and the reaction slows (Mansfield and Meder 2003; Park et al. 2010). Alternatively, increasing substrate heterogeneity has been described as the mechanistic basis of recalcitrance leading to decreasing cellulase activity. As substrate heterogeneity increases, the number of accessible cellulose active sites decrease, leading to decreased surface area and collapsed pore structure that inhibit cellulase movement and activity (Zhang et al. 1999; Våljamäe et al. 1998). Direct testing of these models requires the characterization of cellulose structure evolution. However, the measurement of its numerous non-covalent inter- and intra-molecular bonds presents a technical challenge.

The cellulase field has worked to understand the close relationship between cellulose recalcitrance and cellulase kinetics. Recalcitrance is most often observed indirectly as decreasing soluble sugar release during cellulase reactions (Kostylev and Wilson 2013). However, a deeper insight in cellulose

crystallinity is now more accessible using Fourier transform infrared spectroscopy (FTIR), X-ray diffraction (XRD), and nuclear magnetic resonance (NMR) (Park et al. 2010). Recent advances in atomic force microscopy (AFM) enable cellulose surfaces to be observed directly with low resolution, or indirectly using single enzyme particles (Igarashi et al. 2009; Jeoh et al. 2013). Results from studies using multiple techniques have varied due to structural complexity and sample preparation, with some results correlating crystallinity and cellulase kinetics and other studies showing little or no effect.

FTIR is capable of a rapid and noninvasive quantification of both covalent and non-covalent interactions within cellulose, enabling measurement of crystallinity of the material, expressed as crystallinity indexes. FTIR is also applicable to more complex and industrially relevant cellulose applications, and may be used to investigate the effect of biomass type, pretreatment, and enzyme cocktail synergy on sugar release.

In early work using *Clostridium thermocellum* cellulosomes, bacterial cellulose (BC), and *Valonia ventricosa* cellulose crystals, transmission electron microscopy (TEM) showed significant physical changes to cellulose after hydrolysis. However, XRD and FTIR measurements showed the crystallinity of the residual cellulose unchanged (Boisset et al. 1999). Changes in crystallinity caused by *Cellulomonas fimi* endocellulases, exocellulases, and their synergistic mixtures were measured using both FTIR and solid state NMR (Mansfield and Meder 2003). The results showed that endocellulases increased the overall crystallinity, while exocellulases reduced it. More recently, a report using High Throughput Screening FTIR (HTS-FTIR) has strongly suggested a correlation between cellulose crystallinity and extent of digestion (Corgie et al. 2011). Significant changes to cellulose crystallinity over digestion using *Thermobifida fusca* cellulases (*Tf*Cel6B, *Tf*Cel5A, and *Tf*Cel9A) were observed, and appeared to correlate with cellulase loading.

This paper describes the characterization of residual cellulose using HTS-FTIR to measure cellulose crystallinity after digestion by *T. fusca* cellulases, in an attempt to correlate cellulase kinetic parameters to crystallinity changes. The goal was to validate and expand on the work of Corgie et al. (2011) using the same infrared measurement approach, cellulose substrate, and cellulase loadings. This work builds upon

several reports that show a lack of correlation between cellulose crystallinity and extent of cellulose digestion, using a model cellulose substrate hydrolyzed by either individual cellulases, incomplete synergistic mixtures, or an intact cellulase secretome, (Boisset et al. 1999; Cao and Tan 2002; Chen et al. 2007).

## Materials and methods

### Substrates and enzymes

Cellulose substrates were prepared using methods described elsewhere, summarized in brief here. Bacterial cellulose (a gift from Monsanto, San Diego, CA) was used in this study to mimic conditions used by Corgie et al. (2011). Bacterial cellulose (BC) is more stable in the allomorphic composition ( $I\alpha$  and  $I\beta$  composition) than plant cellulose, making it a more suitable model system for investigating crystallinity changes. It was re-suspended overnight at 4 °C, then washed with Milli-Q water with four cycles of centrifugation and re-suspension. The final concentration of the substrate was determined by measuring dry weight in triplicate. Sodium azide was added to all substrates at a final concentration of 0.02 wt % to prevent microbial contamination. The cellulases used in this study, *Thermobifida fusca* Cel48A, Cel9A, Cel5A, lytic polysaccharide monooxygenase (LPMO) TFAA10B, and ER1 crude supernatant were prepared using previously described methods (Irwin et al. 2003; Kostylev and Wilson 2011; Li et al. 2010). These enzymes were used to represent different hydrolysis mechanisms: Cel48A is an exocellulase (Irwin et al. 2000), Cel9A is a processive endocellulase (Kostylev and Wilson 2014), Cel5A is an endocellulose (Zhang et al. 2000), TFAA10B is a type I LPMO (Forsberg et al. 2014), and ER1 crude supernatant is the mixture of enzymes produced by the protease-deficient mutant of *Thermobifida fusca* (Irwin et al. 2003).

### Hydrolysis assays assembly

Enzyme and substrate stocks (master mixes) were prepared separately at two-fold concentration and combined in Eppendorf protein LoBind 96-well format microplates. Cellulose substrates, ranging in final concentration from 1.25 to 5.0 mg/ml were distributed by manually dispensing the substrate

master mix using wide aperture pipette tips. An equal volume of enzyme master mix, final concentration ranging 10–1000 nM, was added using an Eppendorf EpMotion 5075Vac liquid handling robot, bringing each microplate well to a final volume of 160  $\mu$ l and a final buffer concentration of 50 mM sodium acetate (pH 5.5). Plates were sealed (AB-0745 seals, Fisher Scientific, Hampton, NH), then vortexed briefly on each corner to ensure substrate suspension at the start of incubation. Plates were incubated in a 48-plate tower incubator (StoreX STX40, Liconic US Inc, Woburn, MA) at 50 °C with constant horizontal shaking (150 rpm). Samples were removed at the appropriate reaction times by a Zymark plate handling system (Twister II, PerkinElmer Inc., Waltham, MA). Reactions were immediately stopped by heating to 100 °C for 5 min within a PCR thermocycler heating block (PTC-100, MJResearch Inc., Waltham, MA). The reaction time was set such the drop-off in kinetic rate during the hydrolysis was captured. In addition, enough residual cellulose needed to be available for characterization after reaction.

### Extent of digestion quantification

Hydrolysis samples were centrifuged for 5 min at 4000 rpm (RCF = 3313) to separate residual substrate, then 40  $\mu$ l of supernatant was transferred to a new plate. For complete secondary hydrolysis of short oligosaccharides to glucose, 120  $\mu$ l of excess Novo188  $\beta$ -glucosidase (buffer exchanged with 5 mM NaOAc, pH 5.5, 10% glycerol, 0.22 CBU/ml) (Novozymes, Davis, CA) was added, maintaining the final buffer concentration of 50 mM NaOAc (pH 5.5). A cellobiose standard curve was added to each plate to confirm complete hydrolysis, and plates were incubated for 16 h as described above.

The extent of digestion was determined by quantifying released glucose using the bismuth-catalyzed p-hydroxybenzoic acid (PAHBAH) method of Lever (1977), modified for microscale analysis and validated using existing HPLC quantification methods (Kostylev et al. 2014). The PAHBAH reaction of 120  $\mu$ l PAHBAH reagent added to 40  $\mu$ l of hydrolysate was heated using a PCR thermocycler at 70 °C for 10 min, cooled to 4 °C for 5 min, and finally brought to room temperature as recommended by King et al. (2009). The reaction was transferred to flat bottom polystyrene plates (Costar 9017, Corning Inc., Corning, NY), and

measured at 410 nm using a microplate spectrophotometer (Synergy 2, BioTek Instruments Inc., Winooski, VT). PAHBAH signal was compared to the hydrolyzed G2 standard curve, quantified as units of anhydrous glucose ( $162 \text{ g mol}^{-1}$ ) (Olsen et al. 2014), and extent of digestion was calculated using Eq. 1:

$$\% \text{ Digestion} = \left( \frac{x \mu\text{mol glucose}}{\frac{x \text{mg BC initial}}{\frac{0.162 \text{mg}}{1 \mu\text{mol}}}} \right) \times 100 \quad (1)$$

### Cellulose processing and plating for FTIR

The residual cellulose from hydrolysis was washed and the concentration normalized prior to plating for FTIR analysis. These two steps, together with the lack of internal standard in FTIR measurements, constitute the main methods improvements compared to the experimental protocol used by Corgie et al. (2011). First, the cellulose within the assay hydrolysate was thoroughly re-suspended, using narrow aperture pipette tips, and transferred to a 96-well filter plate (Pall 380  $\mu\text{l}$  0.45  $\mu\text{m}$  filter plate, SUPOR membrane). For comparison of the effect of pipette tip aperture on the reproducibility of BC standard curve crystallinity measurements, either narrow or truncated tips were explored (Supplemental Fig. 1). The liquid fraction was separated by vacuum filtration and stored for digestion yield validation by HPLC. The residual cellulose was re-suspended in Milli-Q water and washed three times on the filter to remove all soluble compounds. In order to normalize the cellulose concentrations, residual cellulose was thoroughly re-suspended in an appropriate volume of Milli-Q water to account for the fraction of cellulose digested during hydrolysis. 50  $\mu\text{l}$  of this suspension was transferred (either manually using a multichannel pipette or using the EpMotion liquid handling system) to clean and dried 96-well silicon FTIR-HTS plates (Bruker Optics, Germany). Each sample biological replicate was plated in triplicate on the FTIR plate. On each plate, a substrate standard curve of known cellulose concentrations was added in triplicate, and a well was left empty for background measurement. After samples were distributed onto the silicon plate, variance in surface tension caused occasional incomplete well coverage, which required manual spreading of the sample to

evenly cover the entire surface. This simple step decreases variance between replicates. Sample plates were placed in a freshly recharged desiccator for gradual drying at least 16 h at room temperature. Drying was completed by heating in a vacuum oven at 60 cm Hg vac. and 70  $^{\circ}\text{C}$  for at least 8 h. The plates were allowed to return to 25  $^{\circ}\text{C}$  prior to measurement.

### FTIR measurement and data processing

All FTIR spectra were collected in transmission mode and atmospheric compensated, between 7000 and 400  $\text{cm}^{-1}$  wavenumbers, 2  $\text{cm}^{-1}$  spectral resolution, and 32 scans per sample using a Bruker Vertex 70 FTIR spectrometer (Bruker Optics, Germany) equipped with a HTS-XT module. Prior to detection, calibration of the equipment was performed according to manufacturer instructions. Two factor zero filling was applied during data collection.

Data processing was performed with the OPUS software package using a self-design macro script. The raw spectra were converted from transmittance to absorbance and cut to remove wavenumbers above 4000  $\text{cm}^{-1}$ . Concave rubber band baseline correction was applied (10 iterations), and the resulting spectra were analyzed without normalization. The intensity values of second derivative peak heights for each sample (used for quantification based on the consistency of signal amplitude after concentration normalization) were used to calculate the three standard crystallinity indexes described in literature. A crystallinity index (CI) is the ratio of a peak related to crystallinity to a peak not representing crystallinity within the same spectrum. Hydrogen bonding intensity (HBI) is the ratio between 3350  $\text{cm}^{-1}$ /1337  $\text{cm}^{-1}$  bands as described by Nada et al. (2000). Lateral order index (LOI) described by Hurtubise and Krassig (1960) and expanded by Nelson and O'Connor (1964) is the ratio between 1427  $\text{cm}^{-1}$ /895  $\text{cm}^{-1}$  bands. Total crystallinity index (TCI) is the ratio between 1373  $\text{cm}^{-1}$ /2900  $\text{cm}^{-1}$  bands as described by Nelson and O'Connor (1964). The resulting values for each sample were imported into OriginPro 2015 (OriginLab, Northampton, MA) for visualization and graphing. The time course reaction kinetics were analyzed by applying the two-parameter power law fit to % digestion data according to Kostylev and Wilson (2013).

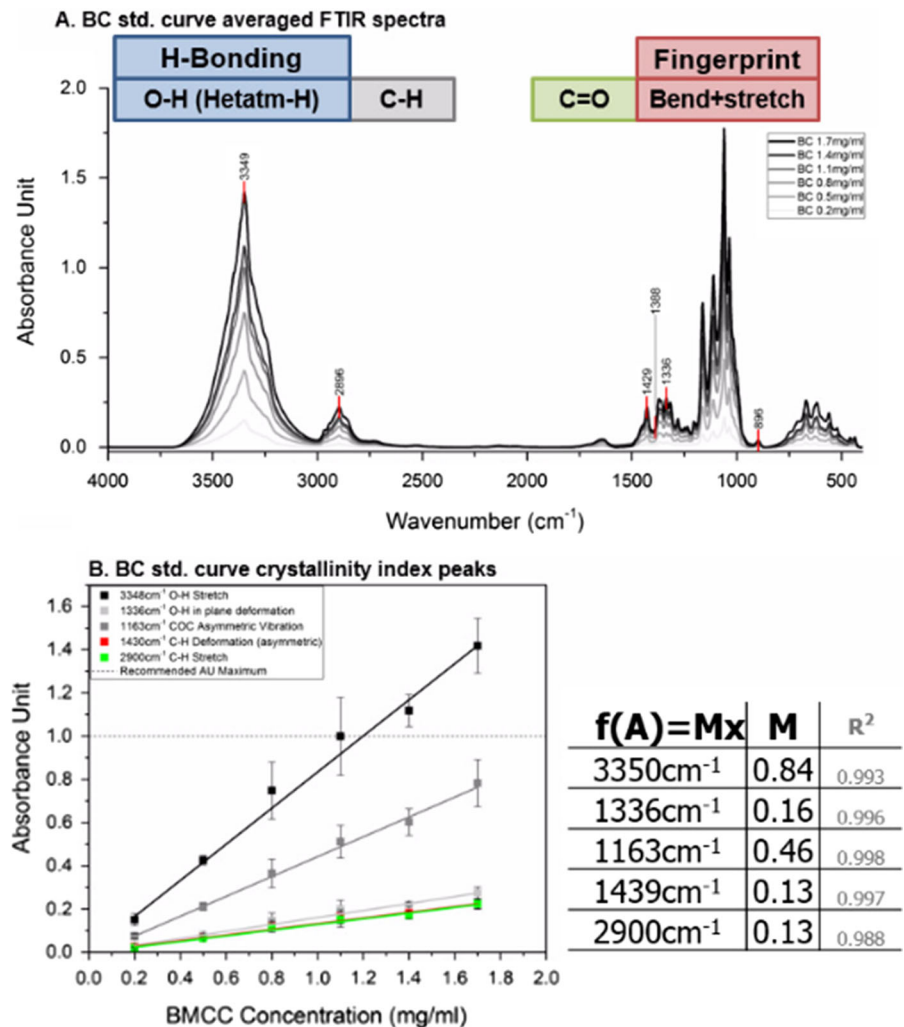
## Results

### Methods improvement

Cellulose samples with varying extents of digestion can only be compared meaningfully using the HTS-FTIR technique when many variables are carefully controlled. Changes to the HTS-FTIR sample preparation methods described by Corgie et al. (2011) were necessary in order to obtain clean raw spectra and reliable measures of cellulose crystallinity. The sample preparation methods were improved to remove extraneous overlapping signals, provide accurate extent of digestion, and correct errors caused by varying cellulose concentration.

The processed bacterial cellulose FTIR spectrum between 4000 and 400  $\text{cm}^{-1}$  contains several characteristic regions serving as landmarks as presented in Fig. 1a. These regions contain the peaks from individual chemical vibrational modes relevant for measuring crystallinity. A representative standard curve of untreated BC spectra is shown in Fig. 1b, showing a BC concentration range from 0.2 to 1.7 mg/ml in 0.3 mg/ml increments. The spectra shown in Fig. 1a closely match previously reported cellulose I FTIR spectra, indicating no alteration of cellulose structure during sample processing (Corgie et al. 2011). At the left of the cellulose FTIR spectrum is the hydrogen bonding region, which extends from 3800 to 3000  $\text{cm}^{-1}$  and contains signals from inter and intra-

**Fig. 1 a** Bacterial cellulose transmission FTIR spectra over the working range (0.2–1.7 mg/ml). **b** Standard curve of peaks essential for crystallinity index calculation



molecular interactions between hydrogen and oxygen. A key interaction is measured in the  $3350\text{ cm}^{-1}$  peak, which results from the hydrogen bonding interaction between the 3OH-O5 adjacent to the  $\beta$ -glycosidic bond of the cellulose I $\alpha$  structure ( $895\text{ cm}^{-1}$ ). Next to this region is the C-H bonding region, which is much narrower, between  $3000$  and  $2800\text{ cm}^{-1}$ , and corresponds to the stretching of C-H moieties. In the middle of the Mid-IR wavenumber range, signals from other heteroatoms such as nitrogen as well as double bonds are absent from spectra of pure cellulose. The most complex region of cellulose FTIR spectra is the fingerprint region from  $1430\text{ cm}^{-1}$  to approximately  $850\text{ cm}^{-1}$ , which contains signals from the numerous  $\text{sp}^3$  single bond vibrational modes. Finally, between  $850$  and  $400\text{ cm}^{-1}$  is the region containing multiple bands corresponding to heavy-atom bending and rotation (Mitchell 1990).

Crystallinity indexes calculated from ratios of individual peak heights depend on the consistency of peak resolution, peak wavenumber, and peak shape over a large concentration range. Peak consistency is especially relevant as critical bonds may change in relative spectral peak height after hydrolysis. Figure 1b demonstrates the cellulose detection range for HTS-FTIR. In this standard curve, the peak shapes of characteristic cellulose signal regions do not change with respect to concentration. The resulting values of individual peaks critical for determining cellulose crystallinity from this standard curve are shown in Fig. 1b. These peaks are consistent in wavenumber position, shape, and have a linear relationship with concentration. Not shown is the smaller  $895\text{ cm}^{-1}$  peak used for calculation of the LOI crystallinity index.

The concentration of cellulose samples used is limited by the maximum signal intensity the FTIR detector can accurately measure. Based on the signal resulting from concentrations shown in Fig. 1b, the working range for BC was determined to be under  $1.25\text{ mg/ml}$  to remain below the manufacturer recommended signal limit of  $1.0\text{ AU}$  (absorbance units) for the maximum peak absorbance. The samples presented in Fig. 1 were processed using narrow aperture pipette tips, one of several method improvements to increase the crystallinity indexes data quality (see Supplemental Fig. 1 where the crystallinity indexes for samples processed with narrow and wide aperture pipette tips at different cellulose concentrations are presented).

The concentration of the cellulose suspension plated in FTIR silicon plates determined the thickness of the cellulose film, and therefore the path length of light through the sample. The influence of cellulose concentration on crystallinity indexes was explored, and resulting data is shown in Supplemental Fig. 1b. While there is a high consistency for the TCI and HBI crystallinity indexes over the working concentration range of the transmission FTIR-HTS measurement approach, the effect of path length on LOI can be seen where LOI decreases with increasing BC concentration. Due to this change in LOI, re-suspension of residual cellulose to similar final concentrations (adjusting for % digestion after buffer exchange) was found to be an essential for meaningful data comparison.

After cessation of cellulose hydrolysis, samples contain several compounds at sufficient concentration to contribute to cellulose FTIR spectral signal: proteins (cellulases), cryoprotectants (glycerol), buffers (acetate), and hydrolysis products (free mono/oligosaccharides). These compounds share chemical bond compositions with cellulose, and thus produce peaks that overlap with those from cellulose vibrational modes. The polar compounds will interact non-covalently with cellulose when dried into the cellulose matrix, inflating certain signals such as the hydrogen bonding region centered at  $3350\text{ cm}^{-1}$ . A buffer exchange and sample washing step was effective at removing soluble hydrolysate compounds to produce a clean spectrum of the residual cellulose. As shown in Supplemental Fig. 2, three washing steps are sufficient to remove soluble sugars from the residual BC. Washing is validated in the resulting FTIR spectra, where characteristic bands from acetate ( $1660$  and  $1560\text{ cm}^{-1}$ ) or protein ( $1700$ – $1500\text{ cm}^{-1}$ ) are absent.

#### Evolution of crystallinity of model BC with digestion by individual *T. fusca* cellulases

Cellulases from the *T. fusca* model system were chosen based on their distinct mechanisms, extensive characterization, and prior investigation of their effect on cellulose crystallinity. Model cellulases were chosen to reproduce and expand on the significant results from Corgie et al. (2011), and to understand how their diverse mechanisms affect cellulose crystallinity. Initial hydrolysis assays were conducted prior to developing the method improvements

described above, and resulting FTIR spectra are highly similar to those presented by Corgie et al. (2011). Cel48A, a classical exocellulase, was used for these methods comparison initially.

The most significant correlation between cellulase digestion and increasing crystallinity observed by Corgie et al. (2011) resulted from digestion by the processive endocellulase Cel9A. To reevaluate the effect of Cel9A digestion on BC crystallinity, the conditions for the Cel9A time course hydrolysis assay were chosen to match the extent of digestion observed by Corgie et al. (2011), as seen in the color-filled diamonds in Fig. 2. The close agreement with prior extent of digestion results indicates that similar enzymes, substrates, and incubation conditions were employed. In this work, a range of eight Cel9A concentrations from 10 to 1000 nM, and two BC substrate concentrations (1.25 and 2.5 mg/ml) were tested. The time course hydrolysis assay for Cel48A and its comparison with the results obtained from Corgie et al. (2011) are presenting in Supplemental Fig. 3 a.

Crystallinity index changes upon BC Cel9A digestion obtained in this work, and the comparison with the results from Corgie et al. (2011) are shown in Fig. 3. (Supplemental Fig. 3b for the crystallinity indexes of BC hydrolysed with Cel48A). Two representative data sets are shown, with similar results of other concentration combinations omitted for clarity. In all conditions, the crystallinity indexes of the residual substrate were not significantly different compared with the BC only negative control. Samples reported by Corgie

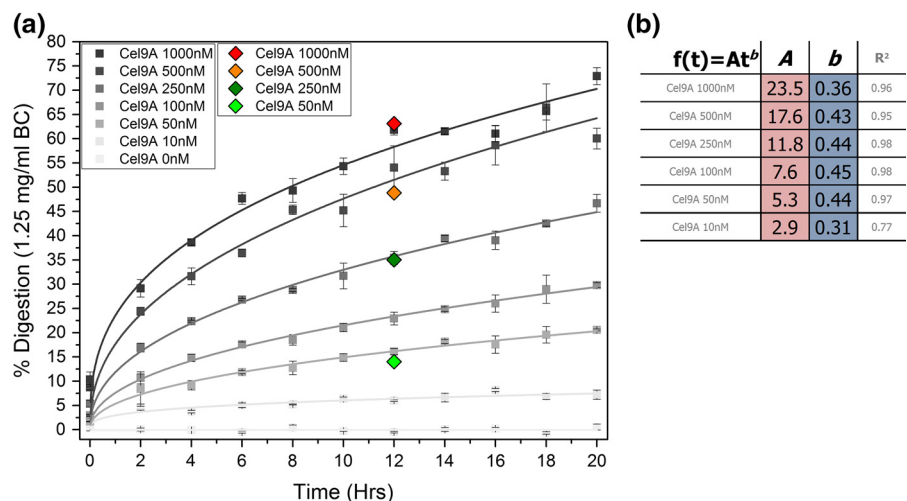
et al. (2011) showed a strong correlation between digestion and crystallinity index ratio values (colored points).

The cleavage activity of lytic polysaccharide monoxygenases (LPMOs) on bacterial cellulose structure was compared with hydrolytic cleavage by the classical endocellulase Cel5A. Two forms of the *T. fusca* type I LPMO TfLPMO10B were tested: full length wild type (WT) and the LPMO catalytic domain (CD) form. It was observed that digestion of BC by either Cel5A or AA10B resulted in no significant change to the three crystallinity indexes as compared to the substrate only negative control (Supplemental Fig. 4).

#### Evolution of crystallinity of model BC with digestion by *T. fusca* ER1 cellulase mixture

To confirm that the lack of crystallinity indexes change after digestion was not caused by the low extent of hydrolysis (Cel48A), or the limitations of a monofunctional cellulase acting alone (Cel9A), *T. fusca* ER1 crude supernatant (a complete high activity cellulase system) was investigated over a wide range of % BC digestion. Cellulase mixtures, including all industrial fungal cocktails, interact synergistically to digest cellulose rapidly. *T. fusca* ER1 crude supernatant is a complex cocktail of many different enzymes, including numerous synergistic cellulases and auxiliary activity enzymes, that breaks down highly crystalline cellulose without experiencing the characteristic kinetic drop-off of individual cellulases

**Fig. 2** Yield of digestion for time course hydrolysis assay of BC (1.25 mg/ml) using Cel9A. **a** Data points shown in diamond colors are those reported by Corgie et al. (2011), showing high agreement with the results from this work (grey scale). **b** Values of the two-parameter nonlinear fit of Cel9A time course digestion values processed according to Kostylev and Wilson (2013). (Color figure online)



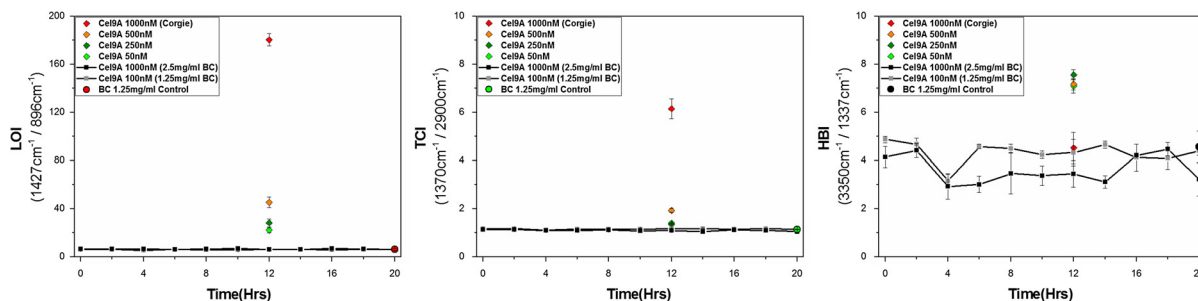


**Fig. 3** FTIR LOI, TCI, and HBI crystallinity index values of two concentrations of Cel9A plotted with respect to time for Cel9A hydrolysis (black and grey values). Colored values with

diamond symbols are those reported by Corgie et al. (2011). Values in large circles at the end of the experiment time are those for BC only controls

(Kostylev and Wilson 2013). Synergistic cooperation likely involves changes to cellulose structure that maximize the activity of the synergistic cellulases.

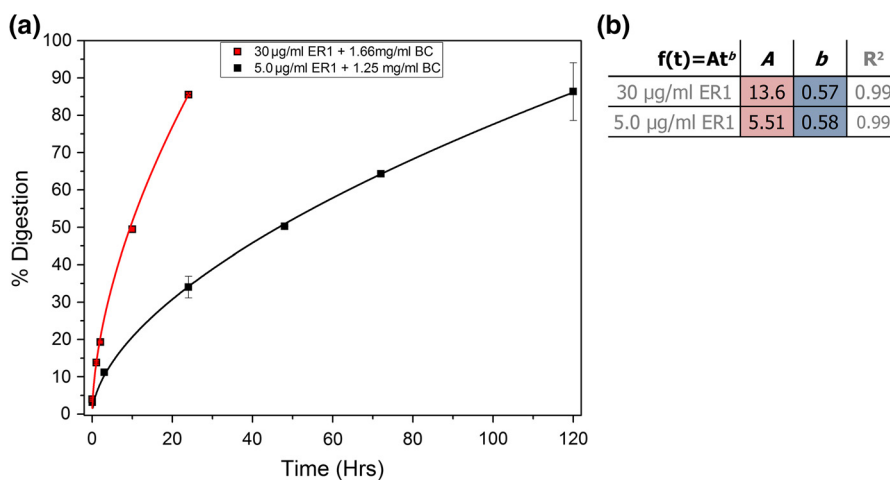
ER1 crude supernatant hydrolysis time course samples with a very high extent of digestion, (Fig. 4) resulted in kinetic parameters agreeing with previously reported values (Kostylev and Wilson 2013).

Quantification of the FTIR spectra of the residual BC after ER1 supernatant digestion either using previously reported methods or updated methods, and their comparison with control BC (without enzyme), are shown in Fig. 5. FTIR spectra collected from residual BC using the updated methods described above show no changes to the HBI or TCI crystallinity indexes (Fig. 5). Compared with results using previous methods, both the control and digested samples with updated methods show very consistent crystallinity index values over time.

### Discussion and integration of this work with the existing literature

The substrate utilized in this study was bacterial cellulose to mimic the conditions used by Corgie et al. (2011) in their experiments. Bacterial cellulose is composed mainly of cellulose I $\alpha$  allomorph, which has implications for crystallinity and enzymatic digestion compared with the cellulose I $\beta$  allomorph dominant in plant cellulose. Corgie et al. (2011) determined the ratio of allomorphs I $\alpha$  and I $\beta$  in the residual cellulose substrate after digestion with different enzymes, finding preferential I $\alpha$  digestion by Cel9A, and I $\beta$  by Cel6B, Cel5A and their mixtures. However, the determination of this cellulose allomorph ratio via deconvolution of the 710–750  $\text{cm}^{-1}$  broad spectral bands was not found reliable to be used in this study, without confidence to conclusively state a negative result.

**Fig. 4** Digestion time course of ER1 crude supernatant on bacterial cellulose. **a** Data is shown using methods of Corgie et al. (2011) (Red) and updated methods (Black). **b** Kinetics parameters for digestion with ER1. (Color figure online)



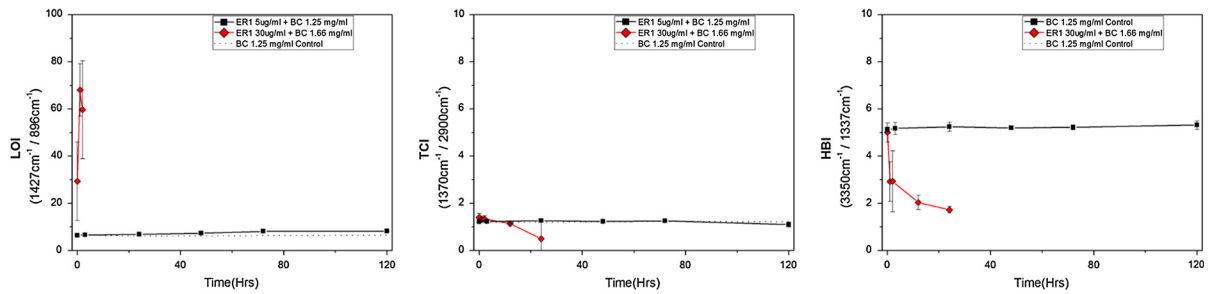


**Fig. 5** LOI, TCI, and HBI crystallinity indexes of residual cellulose after digestion by ER1 crude supernatant. Results for samples prepared using previous methods are shown in red,

results using updated methods are shown in black, and controls without cellulase are shown as black dotted lines. (Color figure online)

During their cleavage of cellulose, cellulases reach a digestibility limit that indicates an accumulation of inhibitory substrate changes. However, these physical changes have not been definitively established. It can be hypothesized that cellulases remove more easily amorphous regions to leave recalcitrant cellulose with increased crystallinity. The exocellulase Cel48A from *T. fusca* is effective in synergistic mixtures, but alone can only digest a small fraction of crystalline cellulose. In contrast, the processive endocellulase Cel9A is the most effective cellulase on crystalline cellulose. Cel9A reaches a higher extent of digestion than exocellulases, and therefore, it must change the substrate in a different way to overcome the increasing recalcitrance. This difference in efficacy makes Cel9A a useful counterpoint to Cel48A to observe changes in crystallinity (see Supplemental Fig. 3).

The results presented in this study indicate that cellulase digestion does not cause significant changes to cellulose crystallinity indexes when the samples are FTIR measured without interferences from other components of the hydrolysate (after buffer exchanged), concentration normalized, gradually dried, and measured without normalization to an internal standard. However, large and reproducible changes to both the raw FTIR spectra and the resulting crystallinity indexes are observed when the previously reported processing methods are used. The most likely causes of these changes are the conversion of ordered cellulose to soluble mono- and oligosaccharide products that remained in the sample to be measured, and the corresponding decreased path length of the lower concentration cellulose sample.

Soluble mono- and oligosaccharides in the sample to measure would be expected to significantly affect the crystallinity indexes of residual cellulose due to the

changed structural interaction of these products with the bulk cellulose. The three crystallinity indexes depend on the relationship between peaks representing bond mobility or non-covalent interactions with those that are unaffected by lattice structure. Free oligosaccharides pack more randomly between the ordered microfibrils of cellulose during drying, resulting in reduced non-covalent interactions while the signal from pyranose ring covalent bonds remained unchanged. This could produce the diminished spectra and changes to crystallinity indexes observed, despite the crystallinity of the residual cellulose remaining unchanged. Therefore, in this study the hydrolysate resulting from the reaction was washed with Milli-Q water and vacuum filtrated three times to remove the elements that could affect the FTIR crystallinity measurements of residual cellulose (mono and – oligosaccharides, buffer, and residual enzyme), as shown in Supplemental Fig. 2a.

The action of individual cellulases are expected to reduce the IR samples path length, as the soluble oligosaccharide products are much smaller and contribute little to the packing of much larger cellulose microfibrils. However, the spectral signal reduction observed in previous reports with low extent of digestion is disproportionate to the amount of soluble products removed (Corgie et al. 2011). This may be explained as digestion induces more compact packing of the cellulose microfibrils. The less ordered and bulky surface chains were removed in these samples, resulting in a shorter path length without significant removal of mass. This change to packing may be entirely uncorrelated with crystallinity of cellulose if reorganization of surface chains results in the same degree of disorder on the individual microfibril scale (a

likely scenario since highly disordered chains would have minimal inter-chain interactions).

Another possibility to explain significant crystallinity index changes for samples with high extent of digestion is the reduced coverage of the well on sampling plates by the residual cellulose. Cellulose samples that fail to cover the well surface would have more stray light, which does not pass through the cellulose. Stray light causes the detector to receive more background light, leading to different effects on bands with different absorptivity (Chalmers 2006). In this work, this effect was avoided by manual spreading the sample to evenly cover the FTIR plate well surface.

This work focused on the evolution of crystallinity of BMCC digested by individual cellulases and a complex cellulase mixture. The rapid drop-off of Cel48A (reducing end directed *T. fusca* exocellulase) activity on BC digestion suggested a rapid enrichment of substrate crystallinity. Though initial results using previous sample preparation for FTIR analysis supported this hypothesis, digestion samples processed with updated methods did not show the same trend (see Supplemental Fig. 3). The processive endocellulase Cel9A provided a test of the correlation between digestion and crystallinity for individual hydrolytic cellulases showing higher digestion yields. Cel9A is an important component of the *T. fusca* cellulase system, with high activity on both amorphous and crystalline cellulose regions. The Cel9A digestion mechanism is an initial endocellulolytic cleavage of a crystalline chain within the cellulose lattice, followed by processive cleavage. Cel9A produces the highest extent of digestion of any single *T. fusca* cellulase on crystalline cellulose, and showed the most significant change to all three crystallinity ratios in previous investigations. The increase of both LOI and TCI, with a decrease to HBI, indicated a significant increase in crystalline fraction in cellulose. This was attributed to preferential digestion of the more disordered cellulose regions prior to engaging highly crystalline substrate. In the current work, Cel9A time course samples were prepared with an extent of digestion matching previously reported digestion values by Corgie et al. (2011), with sugar yields obtained using the PAHBAH method and validated using HPLC quantification. When the residual cellulose was processed using updated methods, the crystallinity indexes did not change significantly during the course of digestion. This may be

explained as Cel9A not exhibiting a preference towards cellulose regions of different crystallinity, or as the cellulose crystallinity equilibrating by some other mechanism. Cel9A plays a major role on the total ER1 crude activity on crystalline cellulose. The next step was to see if the versatility in digestion strategies of ER1 cellulases modifies crystallinity over digestion.

The *T. fusca* secretome ER1 contains hydrolytic cellulases with multiple mechanisms, lytic oxidative enzymes, and proteins of unknown function (Irwin et al. 2003). A rapid, high extent of digestion, approximately 85% within 24 h, is achieved with a high loading of ER1 crude (red squares in Fig. 4). When these residual cellulose samples were prepared for FTIR analysis using the previous methods, significant changes to crystallinity indexes were observed, with a large increase of LOI and a rapid drop of both TCI and HBI. However, when ER1 crude hydrolysis time course samples, at similar extent of digestion, were processed with updated methods, no significant changes were observed in the TCI and HBI crystallinity indexes, suggesting a lack of significant change of the residual BC structural crystallinity over the course of digestion. This observation is in agreement with fluorescence microscopy visualization of structural changes during holocellulose digestion. For pretreated biomass, digestion alters cellulase effectiveness largely through accessibility changes in macrostructure such as porosity and surface area (Donaldson and Vaidya 2017).

Lytic polysaccharide monoxygenases (LPMOs) are used as synergistic components of native or industrial enzyme mixtures at low concentration (often less than 2% of total products). Despite their low extent of BMCC digestion (1% measured by soluble product), they produce a large synergistic effect (Cannella et al. 2012). It is commonly accepted that LPMOs perform oxidative cleavage to degrade crystalline polysaccharides, but the physical changes to the substrate that enable synergism with hydrolytic cellulases are not understood. The amorphogenesis model of LPMO activity was based upon a physical disruption of cellulose crystallinity resulting in a more digestible material (Arantes and Saddler 2010). However, using the same residual cellulose preparation methods for FTIR as with hydrolytic cellulases, no change to cellulose crystallinity was induced by LPMO attack (see Supplemental Fig. 4). This

observation does not support the amorphogenesis model of LPMO attack. In comparison, the classical endocellulase Cel5A is thought to predominately attack more amorphous and solvent exposed cellulose chains. In this work, no change to cellulose crystallinity was observed over the course of digestion.

A different theory to explain cellulose recalcitrance that does not heavily rely on increase of substrate crystallinity needs to be developed. The surface erosion model is the mechanistic explanation that is most in line with these results. This hypothesis proposes the increasing surface complexity as the basis of increasing cellulose recalcitrance, through a mechanism where chains from the more highly ordered crystalline microfiber core become surface chains as digestion proceeds (Väljamäe et al. 1998). This model appears to be supported by microscopy observations of changes to the disorder in cellulose supramolecular structure, after digestion progresses beyond an initial phase of limited cellulase accessibility (Peciulyte et al. 2016). As the chains become more exposed, they may disorder through contact with the solvent, resulting in continual equilibration of crystallinity to the starting value as digestion progresses. According to a surface erosion model, cellulose recalcitrance would not be increased by build-up of ordered crystalline chains, but by the accumulation of disorder on accessible surfaces relative to the starting material (Hu et al. 2015).

While FTIR offers a unique window into cellulose structure, further investigation into the supramolecular changes induced by digestion is warranted. Ongoing work in this space coupling FTIR with orthogonal techniques such as XRD, NMR, and SEM has the potential to reveal important details of these structural changes and their relevance to digesting plant holo-cellulose (Auta et al. 2016). In summary, the results presented in this work are in agreement with the current understanding of cellulose recalcitrance within plant biomass, where recalcitrance is correlated with increasing cellulose complexity rather than cellulose crystallinity.

## Conclusions

The results presented in this work do not support the hypothesis that nonlinear cellulase kinetics on recalcitrant cellulose is due to increased cellulose

crystallinity, as measured by the three most common FTIR crystallinity indexes. The substrate recalcitrance, which inhibits cellulase activity, appears to be a change to cellulose structure that does not involve crystallinity. These combined results suggest that during digestion, the removal of cellulose chains does not affect the substrate crystallinity. This observation is seen regardless of the digestion mechanism of the cellulase used; processive endocellulase (Cel9A), non-processive endocellulase (Cel5A), exocellulase (Cel48A), oxidative cleavage (LPMO), and complete cellulase systems (ER1 crude).

The cellulose digestion yields presented in this work successfully reproduced prior data using similar enzymes and equipment, but methodological changes in analyzing residual cellulose crystallinity produce data that do not support the cellulose crystallinity model of recalcitrance. Current results alter the interpretation of previously presented data, and provide a valuable direction for design of future recalcitrance investigation. Moving toward the goal of biomass deconstruction for fuel and chemicals will require a more nuanced understanding of the subtle changes occurring to the structure of cellulose, and how these changes influence cellulase activity within the context of real biomass substrates.

**Acknowledgments** The authors thank Prof. Larry Walker from Cornell University. Work was funded by a grant from the US Department of Energy BioEnergy Science Center (BESC). The research was supported by a fellowship from Obra Social “La Caixa”.

## References

- Arantes V, Saddler J (2010) Access to cellulose limits the efficiency of enzymatic hydrolysis: the role of amorphogenesis. *Biotechnol Biofuels* 3(4):1–11
- Auta R, Adamus G, Kwiecien M, Radecka I, Hooley P (2016) Production and characterization of bacterial cellulose before and after enzymatic hydrolysis. *Afr J Biotech* 16(10):470–482
- Boisset C, Chanzy H, Henrissat B, Lamed R, Shoham Y, Bayer E (1999) Digestion of crystalline cellulose substrates by the clostridium thermocellum cellulosome: structural and morphological aspects. *Biochem J* 340(3):829–835
- Cannella D, Hsieh C, Felby C, Jørgensen H (2012) Production and effect of aldonic acids during enzymatic hydrolysis of lignocellulose at high dry matter content. *Biotechnol Biofuels* 5(26):1–10
- Cao Y, Tan H (2002) Effects of cellulase on the modification of cellulose. *Carbohydr Res* 337(14):1291–1296

- Chalmers J (2006) Mid-infrared spectroscopy: anomalies, artifacts and common errors. *Handb Vib Spectrosc* 2327–2347
- Chen Y, Stipanovich A, Winter W, Wilson D, Kim Y (2007) Effect of digestion by pure cellulases on crystallinity and average chain length for bacterial and microcrystalline celluloses. *Cellulose* 14:283–293
- Corgie S, Smith H, Walker L (2011) Enzymatic transformations of cellulose assessed by quantitative high-throughput Fourier transform infrared spectroscopy (QHT-FTIR). *Biotechnol Bioeng* 108(7):1509–1520
- Donaldson L, Vaidya A (2017) Visualizing recalcitrance by colocalization of cellulase, lignin, and cellulose in pretreated pine biomass using fluorescence microscopy. *Sci Rep* 7:44386
- Forsberg Z, Mackenzie A, Sorlie M, Rohr A, Helland R, Arvai A, Fijsink V (2014) Structural and functional characterization of a conserved pair of bacterial cellulose-oxidizing lytic polysaccharide monooxygenases. *Proc Natl Acad Sci USA* 111(23):8446–8451
- Hu J, Gourlay K, Arantes V, Van Dyk J, Pribowo A, Saddler J (2015) The accessible cellulose surface influences cellulase synergism during the hydrolysis of lignocellulosic substrates. *Chemoschem* 8(5):901–907
- Hurtubise F, Krassig H (1960) Classification of fine structural characteristics in cellulose by infrared spectroscopy. *Anal Chem* 32(2):177–181
- Igarashi K, Koivula A, Wada M, Kimura S, Penttila M, Samejima M (2009) High speed atomic force microscopy visualizes processive movement of *Trichoderma reesei* cellobiohydrolase I on crystalline cellulose. *J Biol Chem* 284(52):36186–36190
- Irwin D, Zhang S, Wilson D (2000) Cloning, expression and characterization of a family 48 exocellulase, Cel48A, from *Thermobifida fusca*. *Eur J Biochem* 267(16):4988–4997
- Irwin D, Leathers T, Greene R, Wilson D (2003) Corn fiber hydrolysis by *Thermobifida fusca* extracellular enzymes. *Appl Microbiol Biotechnol* 61(4):352–358
- Jeoh T, Santa-Maria MC, O'Dell PJ (2013) Assessing cellulose microfibrillar structure changes due to cellulase action. *Carbohydr Polym* 97(2):581–586
- King B, Donnelly M, Bergstrom G, Walker L, Gibson D (2009) An optimized microplate assay system for quantitative evaluation of plant cell wall-degrading enzyme activity of fungal culture extracts. *Biotechnol Bioeng* 102(4):1033–1044
- Kostylev M, Wilson D (2011) Determination of the catalytic base in family 48 glycosyl hydrolases. *Appl Environ Microbiol* 77(17):6274–6276
- Kostylev M, Wilson D (2013) Two-parameter kinetic model based on a time-dependent activity coefficient accurately describes enzymatic cellulose digestion. *Biochemistry* 52(33):5656–5664
- Kostylev M, Wilson D (2014) A distinct model of synergism between a processive endocellulase (TfCel9A) and an exocellulase (TfCel48A) from *Thermobifida fusca*. *Appl Environ Microbiol* 80(1):339–344
- Kostylev M, Alahuhta M, Chen M, Brunecky R, Himmel M, Lunin V, Wilson D (2014) Cel48A from *Thermobifida fusca*: structure and site directed mutagenesis of key residues. *Biotechnol Bioeng* 111(4):664–673
- Lever M (1977) Carbohydrate determination with 4-hydroxybenzoic acid hydrazide (PAHBAH): effect of bismuth on the reaction. *Anal Biochem* 81(1):21–27
- Li Y, Irwin D, Wilson D (2010) Increased crystalline cellulose activity via combinations of amino acid changes in the family 9 catalytic domain and family 3c cellulose binding module of *Thermobifida fusca* Cel9a. *Appl Environ Microbiol* 76:2582–2588
- Lionetto F, Del Sole R, Cannoletta D, Vasapollo G, Manfazzoli A (2012) Monitoring wood degradation during weathering by cellulose crystallinity. *Materials* 5(10):1910–1922
- Mansfield S, Meder R (2003) Cellulose hydrolysis—the role of monocomponent cellulases in crystalline cellulose degradation. *Cellulose* 10(2):159–169
- Mitchell A (1990) Second-derivative FT-IR spectra of native celluloses. *Carbohydr Res* 197:53–60
- Nada A, Kamel S, El-Sakhawy M (2000) Thermal behavior and infrared spectroscopy of cellulose carbamates. *Polym Degrad Stab* 70(3):347–355
- Nelson M, O'Connor R (1964) Relation of certain infrared bands to cellulose crystallinity and crystal latticed type. Part I. Spectra of lattices types I, II, III, and of amorphous cellulose. *J Appl Polym Sci* 8(3):1311–1324
- Olsen S, Borch K, Cruys-Bagger N, Westh P (2014) The role of product inhibition as a yield-determining factor in enzymatic high-solid hydrolysis of pretreated corn stover. *Appl Biochem Biotechnol* 174(1):146–155
- Park S, Baker J, Himmel M, Parilla P, Johnson D (2010) Cellulose crystallinity index: measurement techniques and their impact on interpreting cellulase performance. *Biotechnol Biofuels* 3(10):1–10
- Peculyte A, Kiskis J, Larson P, Olsson L, Enejder A (2016) Visualization of structural changes in cellulosic substrates during enzymatic hydrolysis using multimodal nonlinear microscopy. *Cellulose* 23:1521–1536
- Väljamäe P, Slid V, Pettersson G, Johansson G (1998) The initial kinetics of hydrolysis by cellobiohydrolases I and II is consistent with a cellulose surface-erosion model. *Eur J Biochem* 253(2):469–475
- Väljamäe P, Kipper K, Pettersson G, Johansson G (2003) Synergistic cellulose hydrolysis can be described in terms of fractal-like kinetics. *Biotechnol Bioeng* 84(2):254–257
- Xu F, Ding H (2007) A new kinetic model for heterogeneous (or spatially confined) enzymatic catalysis: contributions from the fractal and jamming (overcrowding) effects. *Appl Catal A* 317(1):70–81
- Zhang S, Wolfgang D, Wilson D (1999) Substrate heterogeneity causes the nonlinear kinetics of insoluble cellulose hydrolysis. *Biotechnol Bioeng* 66(1):35–41
- Zhang S, Irwin D, Wilson D (2000) Site-directed mutation of non-catalytic residues of *Thermobifida fusca* exocellulase Cel6B. *Eur J Biochem* 267(11):3101–3115